The effect of the novel $HO_2 + NO \rightarrow HNO_3$ reaction channel at South Pole, Antarctica

C.S. Boxe, P.D. Hamer, W. Ford, M. Hoffmann and D.E. Shallcross

Antarctic Science / Volume 24 / Issue 04 / August 2012, pp 417 - 425
DOI: 10.1017/S0954102012000144, Published online: 06 March 2012

Antarctic Science 24(4), 417–425 (2012) © Antarctic Science Ltd 2012 doi:10.1017/S0954102012000144

The effect of the novel $HO_2 + NO \rightarrow HNO_3$ reaction channel at South Pole, Antarctica

C.S. BOXE[1], P.D. HAMER[1], W. FORD[2], M. HOFFMANN[3] and D.E. SHALLCROSS[4]

[1]*Earth and Space Science Division, Jet Propulsion Laboratory, California Institute of Technology, Pasadena, CA 91109, USA*
[2]*Computation and Neural Systems, California Institute of Technology, 1200 East California Boulevard, Pasadena, CA 91125, USA*
[3]*Environmental Science and Engineering, California Institute of Technology, 1200 East California Boulevard, Pasadena, CA 91125, USA*
[4]*School of Chemistry, University of Bristol, Cantock's Close, Bristol BS8 ITS, UK*
boxeman3@gmail.com

Abstract: It is well established that the reaction of HO_2 with NO plays a central role in atmospheric chemistry, by way of OH/HO_2 recycling and reduction of ozone depletion by HO_x cycles in the stratosphere and through ozone production in the troposphere. Utilizing a photochemical box model, we investigate the impact of the recently observed HNO_3 production channel ($HO_2 + NO \rightarrow HNO_3$) on NO_x ($NO + NO_2$), HO_x ($OH + HO_2$), HNO_3, and O_3 concentrations in the boundary layer at the South Pole, Antarctica. Our simulations exemplify decreases in peak O_3, NO, NO_2, and OH and an increase in HNO_3. Also, mean OH is in better agreement with observations, while worsening the agreement with O_3, HO_2, and HNO_3 concentrations observed at the South Pole. The reduced concentrations of NO_x are consistent with expected decreases in atmospheric NO_x lifetime as a result of increased sequestration of NO_x into HNO_3. Although we show that the inclusion of the novel HNO_3 production channel brings better agreement of OH with field measurements, the modelled ozone and HNO_3 are worsened, and the changes in NO_x lifetime imply that snowpack NO_x emissions and snowpack nitrate recycling must be re-evaluated.

Received 6 April 2011, accepted 22 December 2011, first published online 6 March 2012

Key words: boundary layer, ice photochemistry, nitric acid, NO_x, ozone, polar chemistry

Introduction

The South Pole station is located on the central high latitude (~ 3000 m) polar plateau, which is sufficiently inland to avoid the influence of short-lived chemical species that originate from the marine environment. Given Antarctica's huge separation from pollution sources, it was expected to be pristine with very low photochemical activity - an example for clean air conditions (Crawford *et al.* 2001). Given this expectation, it was assumed that concentrations of trace gases (e.g. NO_x ($NO + NO_2$), hydrocarbons, HO_x, O_3, HNO_3 etc.) were low. On the contrary, a series of field campaigns have revealed intense chemical activity as implied by unexpectedly high concentrations of trace gases (e.g. Davis *et al.* 2001), occurring within the Antarctic Boundary Layer (ABL), most notably at the South Pole. The geographical position and meteorology of the South Pole also contributes to this unique chemistry, rather than direct anthropogenic pollution. The low average temperatures during springtime and summertime, ~ 223 and ~ 243 K, respectively, frequently cause temperature inversions at the surface, thus limiting the depth of mixed air and greatly impacting boundary layer chemistry. Compounding this issue, the prevailing wind upon the plateau, down-slope off the continent towards the sea, results in longer plateau residence times for air masses. Thus far, the following chemistry has been discovered: 1) NO_x associated with high ozone (O_3) and NO_y (Crawford *et al.* 2001, Davis *et al.* 2001, 2004, 2008, Dibb *et al.* 2004, Huey *et al.* 2004), 2) higher than expected HO_x (Chen *et al.* 2004, Mauldin *et al.* 2004), and 3) emissions of formaldehyde (HCHO) and hydrogen peroxide (H_2O_2) from the South Pole snowpack (Hutterli *et al.* 2004). These measurements have shown that the South Pole boundary layer can be a highly oxidizing environment. The ABL depth has a strong influence on the photochemical activity present as this governs the mixing volume and, therefore, the impact emissions will have on overlying boundary layer chemistry (Davis *et al.* 2008).

One of the most intriguing aspects of these field campaigns is the high NO (e.g. maximum emission rates of 600 pptv s^{-1} ~ 1.70×10^{10} molecules cm^{-3} s^{-1}) found in the summer at the South Pole (Davis *et al.* 2001), which would normally be associated with suburban pollution. Field studies have shown that nitrate photochemistry at the Arctic and coastal Antarctic snowpack predominantly governs the release of NO_x to the overlying boundary layer, reaching levels up to ~ 200 pptv s^{-1} ~ 5.70×10^9 molecules cm^{-3} s^{-1} (Grannas *et al.* 2007). In addition, laboratory studies have shown that the photolysis of μM NO_3^- (2 and 30 μM NO_3^--doped ice films) on ice produces at most 100 pptv s^{-1} ~ 2.80×10^9 molecules cm^{-3} s^{-1} and ~ 240 pptv s^{-1} ~ 6.80×10^9 molecules cm^{-3} s^{-1} of NO_2, respectively (Cotter *et al.* 2003, Boxe *et al.* 2003, 2005).

Table I. List of all reactions.

$HO_2 + NO \rightarrow OH + NO_2$	(R1a)
$HO_2 + NO \rightarrow HNO_3$	(R1b)
$OH + CO(+O_2) \rightarrow HO_2 + CO_2$	(R2)
$OH + VOCs(+O_2) \rightarrow RO_2 + products$	(R3)
$OH + NO_2 + M \rightarrow HNO_3 + M$	(R4)
$OH + CO,CH_4,NMHCs + O_2 \rightarrow HO_2$	(R5)
$NO_2 + h\nu \rightarrow O(^3P) + O_2$	(R6)
$O(^3P) + O_2 \rightarrow O_3$	(R7)

Nitric oxide (NO) production solely from nitrate photochemistry at the South Pole on snow/ice does not account for 600 pptv s^{-1} ~ 1.70×10^{10} molecules cm^{-3} s^{-1} of NO (Davis *et al.* 2001). It appears that photochemistry and the changing boundary layer height (BLH) contribute to trace gas emissions at the South Pole. Two campaigns have shown that the photochemistry at the South Pole is being driven by the emission of NO_x from the snowpack and the changing BLH (Crawford *et al.* 2001, Davis *et al.* 2004), which in turn determines the concentration of NO_x by altering the mixing volume. A shallower ABL means a smaller mixing volume, therefore, NO_x emissions will produce higher resultant NO_x concentrations (Davis *et al.* 2004). In addition, the 24 hour sunlight exposure of the plateau in conjunction with the enhanced photon flux, due to the high surface albedo, plays an important role in determining the photochemical activity (Lefer *et al.* 2001, Jones & Wolff 2003). The concentration of trace gases in the ABL is also affected by the emissions of HCHO, H_2O_2, oxygenated volatile organic compounds (OVOCs) from the snowpack (Hutterli *et al.* 2004, Frey *et al.* 2005), which have been shown through modelling studies to enhance the HO_x budget (Chen *et al.* 2004) and impact ozone production and OH sequestration. Simultaneously, OVOCs can be HO_x sinks, depending upon environmental conditions. For instance, Hamer *et al.* (2007) showed that up to 3–4 ppbv of the observed ozone results from the oxidation of OVOCs by OH. In addition, the low average temperatures lead to temperature inversions at the surface, thus limiting the depth of mixed air and greatly impacting overlying boundary layer chemistry. Air masses tend to have long plateau residence times, which are due to the prevailing wind upon the plateau, down-slope off the continent towards the sea.

It is well known that $HO_2 + NO \rightarrow OH + NO_2$ (R1a) (Table I) plays a major role in atmospheric chemistry. Recently, $HO_2 + NO \rightarrow HNO_3$ (R1b) (Table I) was discovered in the laboratory (Butkovskaya *et al.* 2005, 2007) and subsequently investigated using the GEOS-CHEM 3-D tropospheric chemical transport model (CTM) (Cariolle *et al.* 2008). The Cariolle *et al.* (2008) study was performed at a global scale with a representation of the atmospheric chemistry mostly for the free troposphere. Therefore, the impact could be different for specific regions, where background species concentrations vary from the mean values produced by GEOS-CHEM. This could be the case in boundary layers, over continents or polluted areas. One specific example is in Antarctica, where GEOS-CHEM specifically lacks any parameterization for the modelling of snowpack NO_x emissions. Hence, given the need for additional snowpack-polar boundary layer chemical modelling (Jacobi & Hilker 2007, Boxe & Saiz-Lopez 2008, 2009, Bock & Jacobi 2010) and given the potentially significant impact on regional-scale boundary layer chemistry, we investigate, via a photochemical box model, the impact of (R1b) on NO_x, HO_x, HNO_3, and O_3 concentrations just above the South Pole snowpack.

Table II. Background concentrations used in the model.

Trace gas	Background free tropospheric concentrations
Ozone	25 ppbv
CO	44 ppbv
CH_4	1.72 ppmv
Ethane*	200 pptv
Propane*	10 pptv
Ethene*	8 pptv
Butane*	5 pptv
Methyl hydroperoxide*	160 pptv
Acetone*	140 pptv
Acetaldehyde*	75 pptv

Ppbv = parts per billion by volume, ppmv = parts per million by volume, pptv = parts per trillion by volume.

*Background concentrations of shorter-lived species are higher than reported for ambient South Pole boundary layer levels. The highly oxidizing nature of the South Pole boundary layer requires that free tropospheric concentrations must be elevated relative to the boundary layer concentrations to maintain the observed ambient boundary layer concentrations.

Model description

The same photochemical box model used in Hamer *et al.* (2007, 2008) was used in the present investigation. This photochemical box model was built using ASAD ('A Self-contained Atmospheric chemistry coDe', Carver *et al.* 1997) and was set up to describe the South Pole boundary layer conditions. The model consists of two vertically stacked boxes of air that mix at a rate such that 10% of the box volume is exchanged with a time step of $\frac{1}{2}$ h. The upper layer of the model mixes with the free tropospheric background concentrations of long-lived species at a rate of 5% per model $\frac{1}{2}$ h time step. The model mechanism has 472 gas phase reactions, representative of 163 species and is based on the Master Chemical Mechanism (Jenkin *et al.* 1997). The mechanism includes inorganic reactions, initial reactions of non-methane hydrocarbons (NMHCs) with OH, NO_3, and O_3, and detailed chemical mechanisms describing the degradation pathways of NMHCs containing up to five carbon atoms. The free tropospheric background concentrations of CO, CH_4, and NMHC were adjusted to be consistent with their respective measured background concentrations at Antarctica. The model achieves these

concentrations via free tropospheric mixing in the upper box. Non-methane hydrocarbon concentrations and other background species used in the model were obtained from the ISCAT 2000 (Investigation of Sulfur Chemistry in Antarctic Troposphere) campaign and the CHABLIS (Chemistry of the Antarctic Boundary Layer and the Interface with Snow) project. CO and CH_4 concentrations were obtained from National Oceanic and Atmospheric Administration South Pole flask data. Given the recent identification of OVOCs (methyl hydroperoxide, acetaldehyde, and acetone) at the South Pole (Frey *et al.* 2005, Hamer *et al.* 2007), their corresponding background concentrations were also added, such that there is a flux of OVOCs into the upper box. All of the free tropospheric background concentrations are specified in Table II. The albedo of the snowpack surface in the model was set at 0.8 (Lefer *et al.* 2001). Nitrate photolysis and NO_x emissions from the snowpack was described by using a prescribed emission ratio of 1:2 for NO with respect to NO_2 (Jones *et al.* 2000, 2001, Cotter *et al.* 2003). This reflects studies of snowpack concentrations of NO_x observed during field campaigns at the South Pole and Neumayer (Crawford *et al.* 2001, Davis *et al.* 2004). The flux of NO_x out of the snowpack is 2.4×10^{10} molecules cm^{-2} s^{-1}. In addition to the snowpack NO_x emissions, fluxes of $O(^3P)$ atoms were included into the lower box in line with Hamer *et al.* (2008) and Yabushita *et al.* (2007). HCHO and H_2O_2 fluxes were added to the model, which were equivalent to their respective fluxes observed at the South Pole (Hutterli *et al.* 2004). A wide range of chemical species are also deposited in the lower box onto the snow. A complete list of the deposited species and the deposition rates used is included in the supplemental material (M. King, personal communication 2004; http://dx.doi.org/10.1017/S0954102012000144).

Model simulations

In all of the simulations the model was run over a 15 day period using the same calendar day (30 December) in order to achieve steady state. All of the results presented represent model values from the 15th day though the model does achieve steady state by the 10th day of the simulation. Initial model concentrations of long-lived species are fixed at their background concentrations for the South Pole site and are maintained in part by the downward fluxes due to the free tropospheric background concentrations presented in Table II. These downward fluxes are sufficient to maintain these long-lived species at their observed concentrations. The spin-up period is sufficiently long to prevent model result sensitivity to short-lived species concentrations. A sensitivity analysis was carried out, where the model was setup to run under two scenarios, using the kinetic rate coefficient data for reaction (R1b). The model was run 15 times using a range of BLHs (500, 400, 350, 300, 250, 200, 150, 125, 100, 75, 60, 50, 40, 35 and 30 m) with a constant NO_x emission of 2.4×10^{10} molecules cm^{-2} s^{-1}. The model produces a range of NO_x concentrations that are consistent with observed ranges. Using this full range of tropospheric BLHs, the model was run using a branching ratio (β) of zero for the 'Base Case' and using $\beta \sim 0.78$ equivalent to 243 K and surface pressure at the South Pole for the perturbed case, run 'β-Rate 1'. To be consistent with the central Antarctic plateau region, the location of the box model was set to the surface at 88°S. This location has a weak diurnal cycle in actinic flux, which is not fully representative of the South Pole, but allows for more stable simulations. Further details of the 'Base Case' model run can be found in Hamer *et al.* (2007) under 'run B' and in Hamer *et al.* (2008) in relation to the '1 x $O(^3P)$ run'.

Reaction (R1a) plays a central role in atmospheric chemistry by way of OH/HO_2 recycling, reduction of ozone depletion by HO_x cycles in the stratosphere, and in ozone production in the troposphere. In the stratosphere this reaction moderates the effectiveness of the cycle involving HO_x radicals, which is an important removal mechanism of ozone (Wayne 2000). In the troposphere this reaction plays a key role in controlling the interconversion between HO_2 and OH radicals through cycles involving OH, CO, and volatile organic compounds (VOCs) (see (R2) and (R3) Table I). The VOCs include methane, NMHCs, and other volatile carbon-containing species. Reaction (R3) is a secondary source of OH radicals as well as the major source of tropospheric ozone, through the conversion of NO and NO_2, followed by the photolysis of NO_2 to NO and $O(^3P)$ atoms. The $O(^3P)$ atoms produced combine with O_2 to produce ozone. The OH and O_3 production rates are, therefore, limited primarily by the chain termination reaction involving OH and NO_2 (see Table I for (R4)).

Reaction (R1b) could be another significant chain termination reaction. To assess the importance of reaction (R1b) in the troposphere, Butkovskaya *et al.* (2007) determined the branching ratio $\beta(T, P)$ or rate constant ratio, $\beta(T, P) = k_{1b}/k_{1a} = (530/T(\mathrm{K})) + (6.4 \times 10^{-4} \times P(\mathrm{torr})) - 1.73$, over the full range of tropospheric pressures and temperatures (i.e. 298 K and 760 torr (Earth's surface) to 220 K and 200 torr (Earth's tropopause)). Consequently, at the Earth's surface $\beta(T, P) \approx 0.5\%$ and in the tropopause region $\beta(T, P) \approx 0.8\%$. Given the significant branching of (R1b) (i.e. $\beta(T, P) \approx 0.78\%$, for $T = 243$ K) at the surface in the central Antarctic plateau region, we conduct photochemical box model simulations with and without the inclusion of (R1b) and assess its impact on NO_x, HO_x, HNO_3, and O_3 concentrations just above the South Pole snowpack. The rate constant k_{1b} was derived from $\beta(T, P)$ by considering the recommended value $k_{1a} = 3.5 \times 10^{-12} \exp(250/T)$ cm^3 $molecule^{-1}$ s^{-1} (Sander *et al.* 2006). This NASA Jet Propulsion Laboratory evaluation panel recommended value and the one recommended by the International Union of Pure and Applied Chemistry (IUPAC) panel (Atkinson *et al.* 2004, updated in 2006 at http://www.iupac-kinetic.ch.cam.ac.uk, accessed June 2006) are very similar, the IUPAC one being higher by only 14% at 200 K and 10% at 300 K.

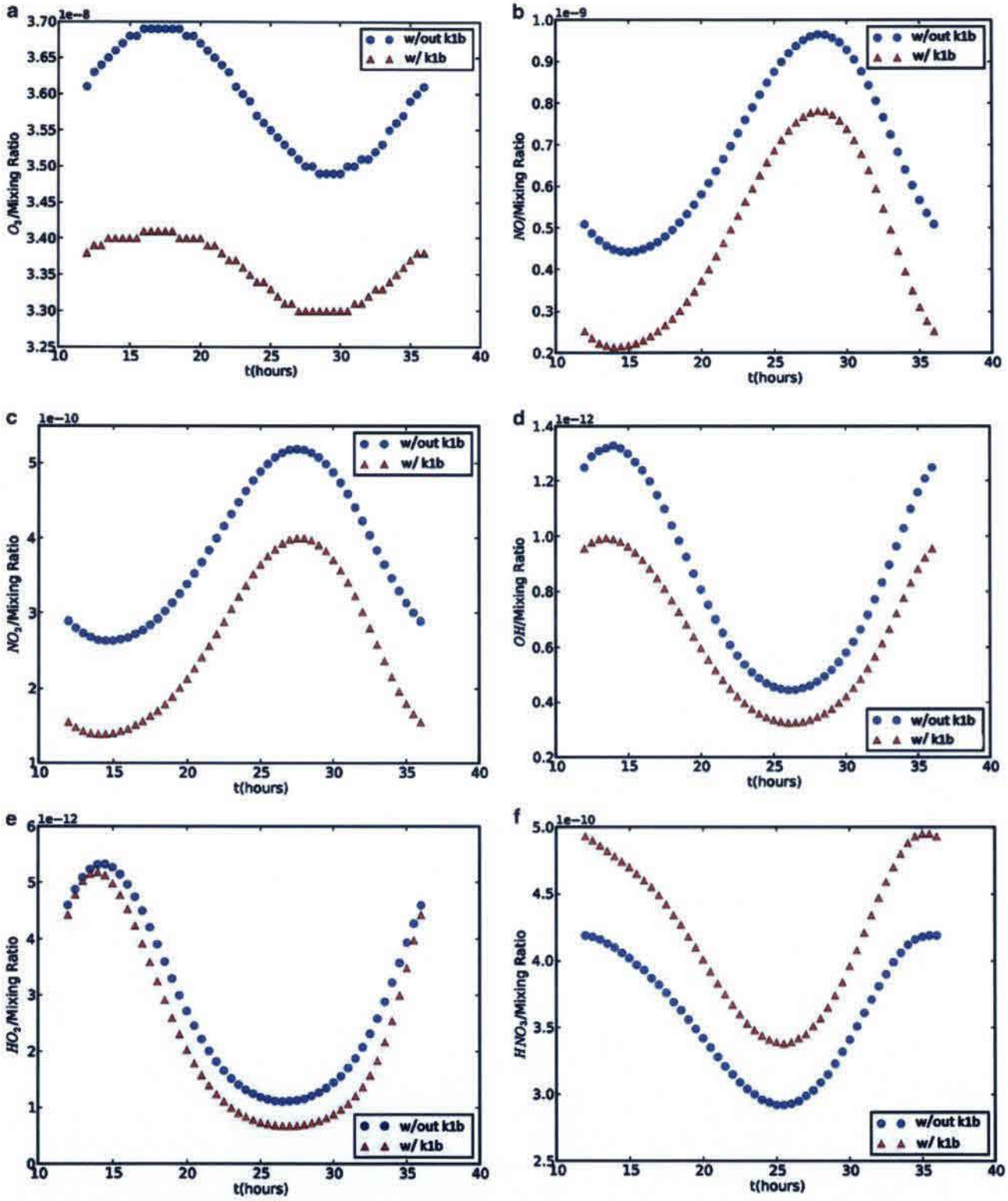

Fig. 1. Diurnal photochemical box model simulations, representative of South Pole conditions of **a.** O_3, **b.** NO, **c.** NO_2, **d.** OH, **e.** HO_2, and **f.** HNO_3 with (red lines) and without (blue lines) $HO_2 + NO \rightarrow HNO_3$ (R1b). All model simulations start at midday. Note: in this figure (k1b) refers to the reaction rate constant of (R1b), which in turn, refers to the same reaction.

Results and discussion

Figure 1a–f displays diurnal photochemical box model simulations at 243 K (representative of the South Pole summer conditions and a BLH of 35 m) of O_3, NO, NO_2, OH, HO_2, and HNO_3 with and without (R1b) starting at midday. The blue profiles denote model simulations without (R1b) included, while the red profiles denote model simulations with (R1b) included. Box model simulations show that O_3 concentration diurnal profiles follow a typical pattern of variability for a polluted environment at the surface, i.e. ozone production beginning in the morning, followed by a peak in ozone concentrations in mid-afternoon, concluding with a decrease in ozone concentrations during the evening. In this simulation this occurs primarily due to the variability in actinic flux and its direct effects upon the chemistry due to the induced changes in snowpack NO_x emissions and photolysis rates of photochemical species. Specifically, increased levels of sunlight lead to enhancements in ozone via reactions (R1a), (R5), (R6) and (R7) (Table I). The decrease in ozone occurs in the evening as the ozone production rate decreases to a point where the combined loss rate for ozone due to deposition and the reaction of O_3 and NO are faster. Ozone production decreases as the levels of HO_x and RO_2 radicals diminish. Including (R1b) causes the net sink of HO_2 and NO to increase and, consequently, the ozone production rate is decreased, leading to decreased ozone concentrations throughout the entire day. HNO_3 follows a similar profile to HO_x species at high NO_x values (i.e. $[NO_x] > \sim 300$ pptv), reduced HO_x and NO_2 concentrations, which results in a decrease in production rate of HNO_3.

The inclusion of (R1b) decreases O_3, NO, NO_2, and OH by 3 ppbv, 200 pptv, 125 pptv, and 0.3 pptv, respectively, from their simulated peak concentrations, while HNO_3 increases by 125 pptv from its peak simulated concentration. Although the peak concentration of HO_2 is unaffected by the

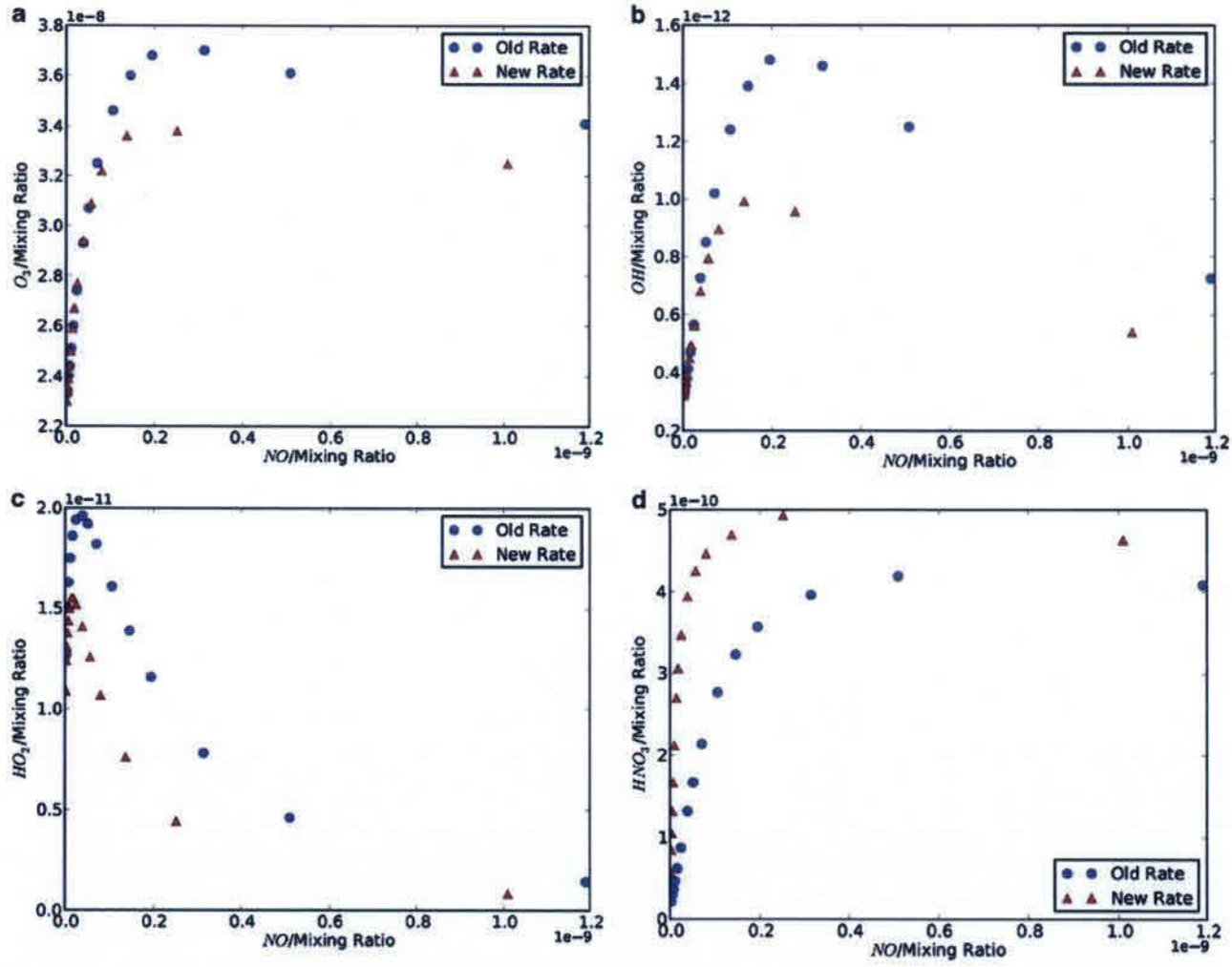

Fig. 2. The mixing ratio dependence of **a.** O_3, **b.** OH, **c.** HO_2, and **d.** HNO_3 on the NO mixing ratio with (red profile) and without (blue profile) the new reaction $HO_2 + NO \rightarrow HNO_3$ (R1b) included. Each data point represents midday concentrations for the individual model run, using different boundary layer heights.

Table III. Modelled concentration ranges for select species with and without the new reaction channel compared to observed species concentration ranges. Note that the variability of these species in the model that leads to these ranges is due to the changes in boundary layer height.

Model species	Range of modelled concentrations with (R1b)	Range of modelled concentrations without (R1b)	Observed concentration range
Ozone	23–34 ppbv	23–37 ppbv	20–45 ppbv
NO	0–1 ppbv	0–1.2 ppbv	1–600 pptv
OH	0.3–1 pptv	0.4–1.5 pptv	0.005–0.24pptv (0.04–0.24 pptv)*
HO_2	11–16 pptv	12.5–20 pptv	2.1–5.3 pptv
HNO_3	50–500 pptv	10–400 pptv	5–68 pptv

*Bracketed range excludes OH values affected by fog events as described by Chen *et al.* (2001).

new chemistry, a small decrease in the lower limit HO_2 is simulated, which is due to the increased efficiency of the $HO_2 + NO \rightarrow HNO_3$ production channel at colder temperatures. Ozone concentrations have reached as high as ~ 45 ppbv during the summer at the South Pole (Crawford *et al.* 2001). The new reaction decreases peak ozone concentrations from ~ 37–34 ppbv, thus worsening the agreement with observations of maximum ozone concentrations at the South Pole. Reaction (R1b) brings better agreement with the peak NO amounts (600 pptv) measured (Davis *et al.* 2001, 2004) during summertime at the South Pole by decreasing peak NO concentrations from ~ 950 to ~ 750 pptv (Hamer *et al.* 2007, 2008). The new reaction reduces NO_2 concentrations from 525–400 pptv. Matsuki *et al.* (2002) provided the only ambient measurements of NO_2 at the South Pole and measure a peak NO_2 concentration of 2.8 ppbv. OH is brought into better agreement with observations (i.e. mean concentrations at the South Pole of 0.09 pptv (2.5×10^6 molecules cm^{-3})) (Mauldin *et al.* 2004). With (R1b) included the mean OH concentration is reduced from ~ 1.10–0.40 pptv (~ 3×10^7 molecules cm^{-3} to ~ 1×10^7 molecules cm^{-3}), which brings our model simulations into better agreement with measured OH in the ABL. A substantial discrepancy remains, however, and this may be due in part to the absence modelled of loss of HO_x due to reaction with NO_x within the snowpack (Hamer *et al.* 2007). Given that the peak HNO_3 concentrations measured at the South Pole is ~ 70 pptv (Huey *et al.* 2004), our photochemical box model simulations still over predict the HNO_3 by an additional 125 pptv. Yet, modelled HNO_3 concentrations and observation agreement may not represent the best test of the new reaction channel since HNO_3 was substantially overestimated before the introduction of (R1b). This overestimation is probably due to the model over predicting HO_x concentrations. HO_2 simulations are incongruent with maximum and mean concentrations of HO_2 measured at the South Pole, ~ 2.50 pptv to 0.04 pptv (~ 7×10^7 and ~ 1×10^6 molecules cm^{-3}), respectively (Chen *et al.* 2001).

Figure 2 displays box model simulations of the mixing ratio dependence of O_3, OH, HO_2, and HNO_3 on the BLH (ranging from 30–500 m, where smaller BLHs lead to elevated NO). Table III displays modelled concentration ranges for select species with and without the new reaction channel compared to observed species concentration ranges. The NO mixing ratios are shown with (red profile) and without (blue profile) the inclusion of reaction (R1b) (Fig. 2). For low concentrations of NO (i.e. < 50 pptv) and high BLHs, ozone increases similarly with NO with and without (R1b) as NO concentrations are not large enough to significantly reduce HO_2, despite the extra loss pathway (Fig. 2a). As NO concentrations exceed 100 pptv, (R1b) starts to influence the loss of HO_2, which in turn leads to less ozone production. At NO > ~ 300 pptv, O_3 starts to decrease (without (R1b)), while at NO > ~ 250 pptv O_3 starts to decrease (with (R1b)). Both profiles exhibit this behaviour as OH start to decrease because of the decreased production of HO_x and NO_2. OH follows a similar concentration dependence on NO as O_3 (Fig. 2b), which is linked to the decrease in OH at NO > ~ 100 pptv due to the increased destruction of HO_2, via (R1b), and decreasing solar radiation, which in turn, caused the production rate of OH to decrease. OH concentrations (without (R1b)) start to decrease at NO > ~ 200 pptv, while it decreases (with(R1b)) at NO > ~ 150 pptv. Figure 2c shows less HO_2 with the inclusion of (R1b) as (R1b) represents an extra sink for HO_2. HO_2 decreases at lower NO concentrations (i.e. at NO > ~ 40 pptv without (R1b) and at NO > ~ 20 pptv with (R1b)), compared to O_3 (i.e. at NO > ~ 300 pptv without (R1b) and at NO > ~ 250 pptv with (R1b)) since the primary pathway leading to the formation of O_3 is preceded by the photolysis of NO_2, which itself is much larger in concentration than HO_2 (e.g. peak NO_2 ~ 500 pptv vs peak HO_2 ~ 5 pptv, see Fig. 1c & e) and is solely not produced from gas phase chemistry but is also emitted readily from the snowpack via nitrate photolysis and diffusion (Hamer *et al.* 2008). HNO_3 concentrations (without (R1b)) start to decrease at NO > ~ 500 pptv while it decreases (with (R1b)) at NO > ~ 250 pptv. HNO_3 production is a function of OH and NO_2 so (at NO > ~ 250 pptv) OH and NO_2 decrease due to (R1b).

Implications

The identification of the new channel for (R1) and its suggested impacts upon the average radical chain length and ozone production at the South Pole present some implications for previously published work regarding this

location and for other cold regions of the atmosphere. Estimates of the photochemical lifetime of NO_x with respect to (R4) are on the order of 3.5 hours, assuming summertime observed OH concentrations 0.09 pptv (2.5×10^6 molecules cm^{-3}) (Mauldin *et al.* 2004) and that $T = 243$ K. The introduction of the new channel reduces the NO_x lifetime with respect to oxidation to HNO_3 to ~ 1 hour with the new channel now dominating the conversion of NO_x to HNO_3 - again utilizing observations of summer HO_2 (Mauldin *et al.* 2004). Thus, existing estimates of snowpack NO_x emissions relying on previous estimates of NO_x lifetime, perhaps, need to be re-evaluated (Wang *et al.* 2008). Such a re-evaluation would need to be revised upwards, which presents a problem for NO_x flux estimates based upon snow radiative transfer models that tend to underestimate snowpack NO_x production rates (Wolff *et al.* 2002, Davis *et al.* 2008) when compared to current observationally derived flux estimates at the South Pole (Oncley *et al.* 2004). This further widens the apparent inconsistency between theoretically required emission burdens at the South Pole, conventional laboratory measurements, and eddy flux covariance estimates of snowpack NO_x emissions (Davis *et al.* 2008). In addition, a significant revision of the photochemical lifetime of NO_x due to the new channel would generally require other observationally constrained inverse estimates of NO_x sources in other environmental regions to be revised. This wider re-evaluation of NO_x lifetime due to the new channel would have particular significance for the emission inversion studies in the upper atmosphere, specifically, with regard to lightning and aircraft NO_x inverse source estimation (Martin *et al.* 2007) since these studies rely on the forward model to accurately describe the NO_x lifetime.

The model simulations including (R1b) result in a substantial increase in boundary layer HNO_3(g), thus over predicting it by over 100 pptv when compared to measurements. This effect would undoubtedly increase surface NO_3^- concentrations via HNO_3(g) deposition. Taking into account an increase in surface NO_3^- concentrations, via an increase in HNO_3(g), would have no effect on HOONO and HONO produced from nitrate photolysis. HOONO is produced from NO_3^- photodecomposition at $\lambda < 280$ nm, via NO_3^{-*}, still, NO_3^{-*} quickly isomerizes back to NO_3^- (Boxe 2005). Concomitantly, as $OH + NO_2 \rightarrow$ HOONO (within the solvent cage of ice), it also quickly isomerizes back to NO_3^- and H^+. HONO production was believed to have a substantial source from NO_3^- photolysis as NO_2^-, a primary product, at low pH readily protonates to form HONO (or nitrous acid in ice). Given that nitrate photochemistry proceeds via two primary photolytic channels (i.e. 10% branching to produce $NO_2^- + O(^3P)$ and 90% branching to produce $NO_2 + O^-$), NO_2^- concentrations will always be smaller than NO_2. For example, snowpack kinetic modelling of nitrate photochemistry by Jacobi & Hilker (2007) revealed that NO_2^- concentrations are always lower than NO_2 concentrations by a factor of approximately three. They also show that in addition to the difference in NO_2^- and NO_2 concentrations, the transfer rate of HONO produced via NO_2^- protonation at low pH would limit any release of HONO produced in the snowpack, whether it is sourced from nitrate photolysis or other chemical or photochemical reaction channels. In other words, Jacobi & Hilker (2007) showed that the high Henry's law constant for HONO at low temperatures (e.g. 930 M atm^{-1} at -20°C, which is 3.6×10^4 higher than the solubility constant for NO_2 at -20°C), dictates its slow transfer from the snowpack to the gas phase.

Conclusions

Here, we examined the effect of the new reaction channel, $HO_2 + NO \rightarrow HNO_3$ (R1b) at the South Pole, Antarctica using a photochemical box model. The inclusion of this reaction decreases O_3, NO, NO_2, OH, and HO_2 and increases HNO_3. The decrease in O_3 from 37–34 ppbv worsens the agreement between the model and the highest O_3 concentrations observed at the South Pole (45 ppbv), which are associated with *in situ* photochemical production. As the mean concentration of OH at the South Pole is 2.5×10^6 molecules cm^{-3}, our box model simulations brings OH into better agreement with observations since OH is reduced from 1×10^7 to 8×10^6 molecules cm^{-3}. Box model simulations of HO_2 are incongruent with maximum and mean concentrations of HO_2 measured at the South Pole, ~ 7×10^7 and ~ 1×10^6 molecules cm^{-3}, respectively. Given that peak measured HNO_3 concentration measured at the South Pole is 70 pptv, our box model simulations still over predict it by an additional ~ 130 pptv. The reduced concentrations of NO_x, as a result of the application of the new channel, are consistent with expected decreases in atmospheric NO_x lifetime as a result of increased sequestration of NO_x into HNO_3. We also show here that without (R1b) current models will overestimate NO_x concentrations at the ABL, which has the following implications: 1) given that previous studies investigating snowpack emissions of NO_x have relied upon accurate and comprehensive determinations of NO_x losses in this environment, our result implies that NO_x snowpack emissions are larger than currently reported, 2) current estimates of the nitrate recycling factor again rely upon accurate characterization of NO_x, and therefore, current estimates are probably too low, and 3) the changes in NO_x lifetime imply that snowpack NO_x emissions and snowpack nitrate recycling must be re-evaluated. Further analysis is required to reduce the degree of incongruence. Our box model simulations of the concentration dependence of OH, O_3, HO_2, and HNO_3 on NO with the new reaction included, overall, show a decrease in OH, O_3, and HO_2 and an increase in HNO_3. Lastly, this new reaction should be further explored and validated experimentally for potential consideration and inclusion in the latest 'Chemical kinetics

and photochemical data for use in atmospheric studies evaluation' handbook.

Acknowledgements

Paul Hamer was supported by an appointment to the NASA Postdoctoral Program at the Jet Propulsion Laboratory, administered by Oak Ridge Associated Universities through a contract with the National Aeronautics and Space Administration (NASA). The work described here was performed at the Jet Propulsion Laboratory, California Institute of Technology, under contracts with NASA. The constructive comments of the reviewers are gratefully acknowledged.

Supplemental material

A Supplemental table will be found at http://dx.doi.org/10.1017/S0954102012000144.

References

Atkinson, R., Baulch, D.L., Cox, R.A., Crowley, J.N., Hampson, R.F., Hynes, R.G., Jenkin, M.E., Rossi, M.J. & Troe, J. 2004. Evaluated kinetic and photochemical data for atmospheric chemistry: volume I - gas phase reactions of O_x, HO_x, NO_x and SO_x species. *Atmospheric Chemistry and Physics*, **4**, 1461–1738.

Bock, J. & Jacobi, H.W. 2010. Development of a mechanism for nitrate photochemistry in snow. *Journal of Physical Chemistry A*, **114**, 1790–1796.

Boxe, C.S. 2005. *Nitrate photochemistry and interrelated chemical phenomena in ice: influence of the quasi-liquid layer (QLL)*. PhD thesis, California Institute of Technology, 225 pp. [Unpublished.]

Boxe, C.S. & Saiz-Lopez, A. 2008. Multiphase modeling of nitrate photochemistry in the quasi-liquid layer (QLL): implications for NO_x release from the Arctic and coastal Antarctic snowpack. *Atmospheric Chemistry and Physics*, **8**, 4855–4864.

Boxe, C.S. & Saiz-Lopez, A. 2009. Influence of thin liquid films on polar chemistry: implications for Earth and planetary science. *Polar Science*, **3**, 73–81.

Boxe, C.S., Colussi, A.J., Hoffmann, M.R., Tan, D., Mastromarino, J., Case, A.T., Sandholm, S.T. & Davis, D.D. 2003. Multiscale ice fluidity in NO_x photodesorption from frozen nitrate solutions. *Journal of Physical Chemistry A*, **107**, 11 409–11 413.

Butkovskaya, N.I., Kukui, A. & Le Bras, G. 2007. HNO_3 Forming channel of the $HO_2 + NO$ reaction as a function of pressure and temperature in the ranges of 72–600 torr and 223–323 K. *Journal of Physical Chemistry A*, **111**, 9047–9053.

Butkovskaya, N.I., Kukui, A., Pouvelse, N. & Le Bras, G. 2005. Formation of nitric acid in the gas-phase $HO_2 + NO$ reaction: effects of temperature and water vapor. *Journal of Physical Chemistry A*, **109**, 6509–6520.

Cariolle, D., Evans, M.J., Chipperfield, M.P., Butkovskaya, N., Kukui, A. & Le Bras, G. 2008. Impact of the new HNO_3-forming channel of the $HO_2 + NO$ reaction on tropospheric HNO_3, NO_x, HO_x and ozone. *Atmospheric Chemistry and Physics*, **8**, 1–8.

Carver, G.D., Brown, P.D. & Wild, O. 1997. The ASAD atmospheric chemistry integration package and chemical reaction database. *Computer Physics Communications*, **105**, 197–215.

Chen, G. *et al.* 2001. An investigation of South Pole HO_x chemistry: comparison of model results with ISCAT observations. *Geophysical Research Letters*, **28**, 3633–3636.

Chen, G. *et al.* 2004. A reassessment of HO_x South Pole chemistry based on observations recording during ISCAT 2000. *Atmospheric Environment*, **38**, 5451–5461.

Cotter, E.S.N., Jones, A.E., Wolff, E.W. & Bauguitte, S.J.-B. 2003. What controls photochemical NO and NO_2 production from Antarctic snow? Laboratory investigation assessing the wavelength and temperature dependence. *Journal of Geophysical Research*, 10.1029/2002JD002602.

Crawford, J.H. *et al.* 2001. Evidence for the photochemical production of ozone at the South Pole surface. *Geophysical Research Letters*, **28**, 3641–3644.

Davis, D., Chen, G., Buhr, M., Crawford, J., Lenschow, D., Lefer, B., Shetter, R., Eisele, F., Mauldin, L. & Hogan, A. 2004. South Pole NO_x chemistry: an assessment of factors controlling variability and absolute levels. *Atmospheric Environment*, **38**, 5375–5388.

Davis, D. *et al.* 2001. Unexpected high levels of NO observed at South Pole. *Geophysical Research Letters*, **28**, 3625–3628.

Davis, D. *et al.* 2008. A reassessment of Antarctic plateau reactive nitrogen based on ANTCI 2003 airborne and ground based measurements. *Atmospheric Environment*, **42**, 2831–2848.

Dibb, J.E., Huey, L.G., Slusher, D.L. & Tanner, D.J. 2004. Soluble reactive nitrogen oxides at South Pole during ISCAT 2000. *Atmospheric Environment*, **38**, 5399–5409.

Frey, M.M., Stewart, R.W., McConnell, J.R. & Bales, R.C. 2005. Atmospheric hydroperoxides in West Antarctica: links to stratospheric ozone and atmospheric oxidation capacity. *Journal of Geophysical Research*, 10.1029/2005JD006110.

Grannas, A. *et al.* 2007. An overview of snow photochemistry: evidence, mechanisms, and impacts. *Atmospheric Chemistry and Physics*, **7**, 4329–4373.

Hamer, P.D., Shallcross, D.E. & Frey, M.M. 2007. Modelling the impact of oxygenated VOC and meteorology upon the boundary layer photochemistry at the South Pole. *Atmospheric Science Letters*, **8**, 14–20.

Hamer, P.D., Shallcross, D.E., Yabushita, A. & Kawasaki, M. 2008. Modelling the impact of possible snowpack emissions of $O(^3P)$ and NO_2 on photochemistry in the South Pole boundary layer. *Environmental Chemistry*, **5**, 268–273.

Huey, L.G. *et al.* 2004. CIMS measurements of HNO_3 and SO_2 at the South Pole during ISCAT 2000. *Atmospheric Environment*, **38**, 5411–5421.

Hutterli, M.A., McConnell, J.R., Chen, G., Bales, R.C., Davis, D.D. & Lenschow, D.H. 2004. Formaldehyde and hydrogen peroxide in air, snow and interstitial air at South Pole. *Atmospheric Environment*, **38**, 5439–5450.

Jacobi, H.-W. & Hilker, B. 2007. A mechanism for the photochemical transformation of nitrate in snow. *Journal of Photochemistry and Photobiology A Chemistry*, **185**, 371–382.

Jenkin, M.E., Saunders, S.M. & Philling, M.J. 1997. The tropospheric degradation of volatile organic compounds: a protocol for mechanism development. *Atmospheric Environment*, **31**, 81–104.

Jones, A.E. & Wolff, E.W. 2003. An analysis of the oxidation potential of the South Pole boundary layer and the influence of stratospheric ozone depletion. *Journal of Geophysical Research*, 10.1029/2003JD003379.

Jones, A.E., Weller, R., Wolff, E.W. & Jacobi, H.W. 2000. Speciation and rate of photochemical NO and NO_2 production in Antarctic snow. *Geophysical Research Letters*, **27**, 345–348.

Jones, A.E. *et al.* 2001. Measurements of NO_x emissions from the Antarctic snowpack. *Geophysical Research Letters*, **28**, 1499–1502.

Lefer, B.L., Hall, S.R., Cinquini, L. & Shetter, R.E. 2001. Photolysis frequency measurements at the South Pole during ISCAT-98. *Geophysical Research Letters*, **28**, 3637–3640.

Martin, R.V., Sauvage, B., Folkins, I., Sioris, C.E., Boone, C., Bernath, P. & Ziemke, J. 2007. Spaced-based constraints on the production of nitric oxide by lightning. *Journal of Geophysical Research*, 10.1029/2006JD007831.

MATSUKI, H., YOSHIKAWA, K.J., YANAGISAWA, Y. & KASUGA, H. 2002. Measurement of atmospheric NO_2 concentrations in Antarctica with NO_2 filter badge and tube. *Tokai Journal of Experimental and Clinical Medicine*, **27**, 35–42.

MAULDIN, L., KOSCIUCH, E., HENRY, B., EISELE, F., SHETTER, R., LEFER, B., CHEN, G., DAVIS, D., HUEY, G. & TANNER, D. 2004. Measurements of OH, $HO_2 + RO_2$, H_2SO4, and MSA at the South Pole during ISCAT 2000. *Atmospheric Environment*, **38**, 5423–5437.

ONCLEY, S.P., BUHR, M., LENSCHOW, D.H., DAVIS, D. & SEMMER, S.R. 2004. Observations of summertime NO fluxes and boundary-layer height at the South Pole during ISCAT 2000 using scalar similarity. *Atmospheric Environment*, **38**, 5389–5398.

SANDER, S.P. *et al.* 2006. *Chemical kinetics and photochemical data for use in atmospheric studies.* Evaluation no. 15. JPL Publication 06-02. Pasadena, CA: NASA. http://jpldataeval.jpl.nasa.gov/pdf/JPL_15_AllInOne.pdf.

WANG, Y.H., CHOI, Y., ZENG, T., DAVIS, D., BUHR, M., HUEY, L.G. & NEFF, W. 2008. Assessing the photochemical impact of snow NO_x emissions over Antarctica during ANTCI 2003. *Atmospheric Environment*, **42**, 2849–2863.

WAYNE, R.P. 2000. *Chemistry of atmospheres*. Oxford: Oxford University Press, 806 pp.

WOLFF, E.W., JONES, A.E., MARTIN, T.J. & GRENFELL, T.C. 2002. Modelling photochemical NO_x production and nitrate loss in the upper snowpack of Antarctica. *Geophysical Research Letters*, 10.1029/2002GL015823.

YABUSHITA, A., KAWANAKA, N., KAWASAKI, M., HAMER, P.D. & SHALLCROSS, D.E. 2007. Release of oxygen atoms and nitric oxide molecules from the ultraviolet photodissociation of nitrate adsorbed on water ice films at 100 K. *Journal of Physical Chemistry A*, **111**, 8629–8634.